Chemical Composition Analysis and Prediction of Tobacco

Saijiao Wang

Taizhou Radio & TV University, Taizhou 318000, China
wsjxf6666@163.com

In order to study the application of digital image processing technology in chemical composition prediction, we have verified the detection of nicotine content in different stages of tobacco. Taking the tobacco leaves at different stages in the baking process of flue-cured tobacco as the research object, the image processing technology was used to extract the image parameters of tobacco leaves at different stages, and the BP neural network was used to establish the prediction model to achieve non-destructive testing. The final prediction results show that the model is feasible to predict the nicotine index at different stages of the baking process according to the color eigenvalues and texture eigenvalues of the tobacco leaves. The prediction results are in line with the actual situation, and the model has certain practical value. This confirms the application value of digital image processing technology.

1. Introduction

The image treatment technology simulates the human visual system and extracts the image information about the objective objects by the computer. On this basis, it reaches a quantitative description on these objects after processing and computing them (Saadat et al., 2012; Galiza and Ferreira, 2013). This paper takes a dive into the application of digital image processing technology in chemical composition prediction. Here is the example for tobacco component detection.

The quality evaluation system of tobacco mainly involves physical properties, sensory quality, appearance quality, chemical composition and safety (Gajewski et al., 2018; Lin et al., 2015). The total chemical composition of the identified flue gas and tobacco reached 5,868, and the composition of the tobacco is complicated. Tobacco is a crop that is mainly used for smoke intake. The spate of aroma produced by the burning of tobacco gives people a sense of pleasure (Leventhal et al., 2015; De Genna et al., 2017). Up till now, there are a large number of studies on the chemical composition and sensory quality of tobacco. Tobacco experts attempted to directly evaluate the tobacco quality using the chemical composition of tobacco leaves.

Tobacco is now still regarded as the best free gifts that convey affection to and build a relationship with others in the tobacco purchase process in China. Such acts will not only cause economic losses to the tobacco growers and dampen their enthusiasm for planting it, but also bring immeasurable losses to the country. Today, the image treatment technology emerges in response to intelligent classification of tobacco leaves. This test extracts the tobacco color and texture information with the image vision technology, and establishes the BP neural network recognition system to analyze the chemical components in the tobacco during baking (Liang and Hu, 2015; Spoerer et al., 2017). Based on the objective values of the tobacco image color and texture, it is analyzed what's the intrinsic relationship between the appearance characteristics and the chemical composition of tobacco. We attempt to eliminate the uncertainty of the man-made subjective factors during the tobacco baking process, and seek an objective and intelligent method for flue-cured tobacco, accurately and quickly realize the judgment on the main chemical components in the tobacco baking process, thus provide the clues to the application of the image treatment technology in the NDT (Nondestructive Testing) of chemical components in the tobacco baking process.

2. Experiments

2.1 Image capture

The image acquisition is achieved by an image vasculum (Figure 1), 140cm × 90cm × 40cm, whose periphery is blocked with black film, on the top of which, a digital camera is secured. There are 2 ring light-emitting diodes as an illumination source. The tube diameter is equivalent to the vasculum in order to ensure that the light in it is even, and the background is white sample loading table.
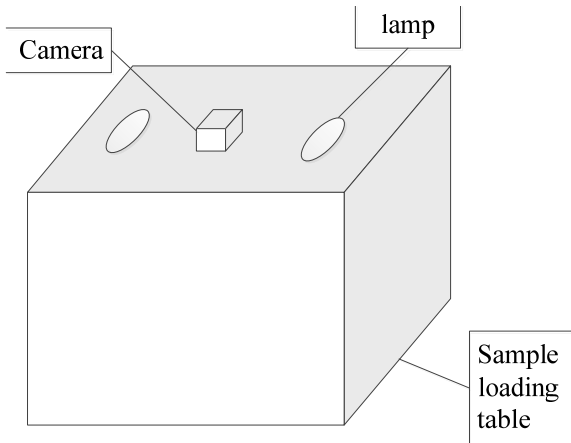

Figure 1: Sample platform

2.2 Extraction of Image features

Image feature extraction is a crosscutting discipline. In this process, mathematics, physics, computer science and many other subjects will often be involved (Romero and Camps-Valls, 2016).

The color eigenvalue is a quantitative description for the color features of all or part of the image. There are two color models commonly used now: the most commonly used one is the RGB model, where individual component is represented by an 8-bit binary integer; the other is the HSV color space model, where the hue (H) indicates different colors; the saturation (S) indicates whether the color is light or shade, and the Value (V) indicates how the color tone seems like. The schematic diagrams of the two models are shown in Figure 2 and 3. The RGB color space model represents the image color information more inaccurately. In current time, the I-ISV color space model is often applied for the image and video capture devices, so that it is required to convert the RGB color space into the HSV color space. For any set of values R, G, B in the range [0,1], convert it into H, S, and V by the formulas
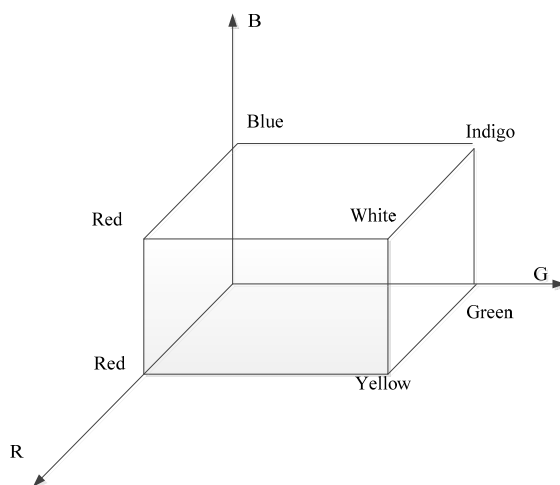

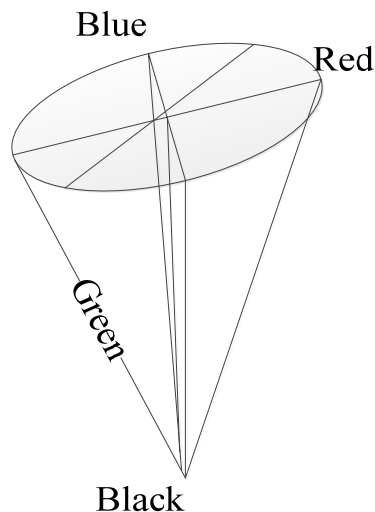*Figure 2: RGB unit cube in a two-dimensional Cartesian color system*

Figure 3: HSV color space model

$$H = \arccos\{\frac{[(R-G)+(R-B)]/2}{\sqrt{[(R-B)^2+(R-B)(R-G)]}}\}$$ (1)

$$S = 1 - \frac{3}{(G+B+G)}[\min(R,G,B)]$$ (2)

$$V = \frac{R+G+B}{3}$$ (3)

The average value of each parameter is

$$\bar{H} = \frac{1}{N}\sum_{i=1}^{N} H_i$$ (4)

$$\bar{S} = \frac{1}{N}\sum_{i=1}^{N} S_i$$ (5)

$$\bar{V} = \frac{1}{N}\sum_{i=1}^{N} V_i$$ (6)

Where: $\bar{H}$ is the average value of the hue; $\bar{S}$ is the average value of the saturation; $\bar{V}$ is the average value of the brightness; H, S, V respectively represent the hue, saturation and brightness of each pixel of the flue-cured tobacco; N is the number of pixels that the flue-cured tobacco covers in the image.

2.3 Extraction of texture features

In this paper, the gray level co-occurrence matrix is used to extract the image texture features since it can reflect the direction of the image texture, the adjacent spacing and the variation magnitude (Beura et al., 2015; Nayak et al., 2016). 4 types of common feature statistics are selected from 5 feature parameters in gray level co-occurrence matrix to extract the texture features of the tobacco image:
Angular second moment:

$$W_1 = \sum_{i=0}^{i-1}\sum_{j=0}^{l-1} p^2(i,j,d,\theta)$$ (7)

Entropy:

$$W_2 = \sum_{i=0}^{i-1} \sum_{j=0}^{l-1} p(i,j) \times \lg p(i \times j) \tag{8}$$

Inverse difference moment:

$$W_3 = \sum_{i=0}^{i-1} \sum_{j=0}^{l-1} \frac{p(i,j,d,\theta)}{1+(i-j)^2} \tag{9}$$

Relevancy:

$$W_4 = \sum_{i=0}^{i-1} \sum_{j=0}^{l-1} \frac{(i \times j \times p(i,j,d,\theta) - u_1 \times u_2)}{d_1 \times d_2} \tag{10}$$

Where,

$$u_1 = \sum_{i=0}^{i-1} \sum_{j=0}^{l-1} p(i,j), u_2 = \sum_{i=0}^{i-1} i \sum_{j=0}^{l-1} p(i,j) \tag{11}$$

$$d_1^2 = \sum_{i=0}^{i-1} (i-u_1)^2 \sum_{j=0}^{l-1} p(i,j), d_2^2 = \sum_{i=0}^{i-1} (j-u_2)^2 \sum_{j=0}^{l-1} p(i,j) \tag{12}$$

The angular second moment is the sum of the squares of the pixel values in the gray level co-occurrence matrix, reflecting what the image gray distribution uniformity and texture thickness seem like. The greater the value, the coarser the texture; the entropy is the measurement of the information quantity that the image has, indicating how complex the texture looks. If there is no texture, the entropy is 0; the inverse difference moment is to measure the size of the local variation in the image texture, the more regular the texture, the greater the value; the relevancy represents how similar the elements in the gray level co-occurrence matrix are in the row or column direction, If the image texture is more regular in a certain direction, the greater its value.

3. Data analysis

3.1 BP neutral network

BP neural network is a learning method of error back propagation with adaptive and self-learning capacities (Wang et al., 2016; Sun and Wang, 2018; Huang et al., 2014). Its computation process includes forward information propagation and error back propagation. It has the most basic constituent unit, that is, the neuron. The neural network topology includes the input layer, hidden layer, and the output layer.
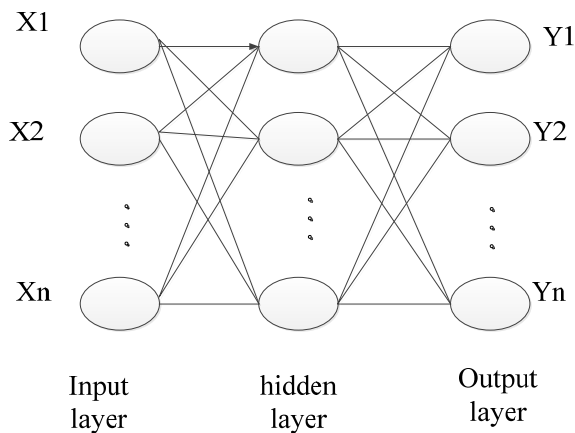

Figure 4: BP neural network structure

The neuron in the input layer receives input information and transmits it to one or more hidden layers, which in turn send processed data to the output layer for further processing. Till now, a forward learning process is completed; when the results output by the output layer does not match the expected values, the error back propaganda is accessed. The network corrects the weight of individual layer according to the error gradient, and in turn via the output layer, the hidden layer and the input layer. In doing so, the error back propagation completes a cycle. Repeat the forward information propagation and error back propagation, the weights continuously get corrected, and the network training is finished. In the end, the tolerance of preset error and requirement for training procedure are met. For a simplified network structure diagram of BP neural network, refer to Figure 4.

3.2 Results and analysis

The optimized network training error curve is shown in Figure 5 below. It can be seen that the error curve predicted by the BP neural network has a faster convergence, and the number of network training steps is 400.
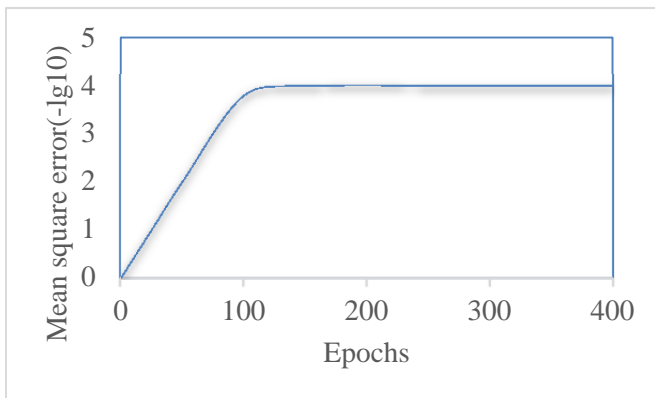

Figure 5: BP neural network prediction error curve

The obtained 240 samples are divided into six baking phases: fresh tobacco, 38 °C, 42 °C, 45 °C, 55 °C and baked tobacco. The network model training and simulation are performed for the nicotine content in different baking phases, and a statistical analysis on the real and predicted values. The results are shown in Figure 6.
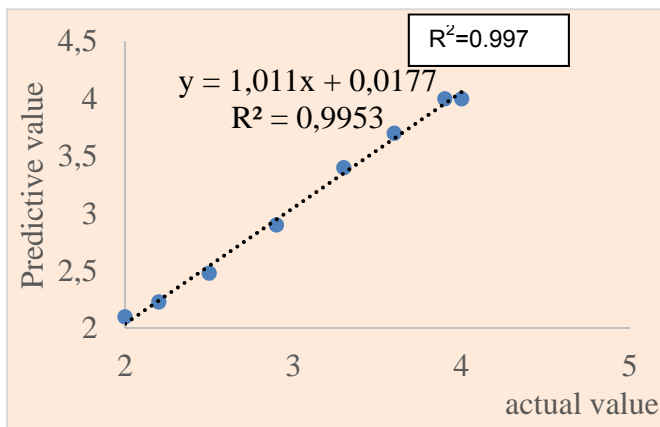

Figure 6: Statistical regression analysis of real and predicted values

According to the regression analysis on the predicted and measured values of the network output, there is a good correlation between the predicted and measured values of network, and the correlation coefficient R is above 0.9. It is suggested that the predicted value is very close to the measured value.

4. Conclusion

In this paper, the BP chemical network with very strong nonlinear mapping ability is used to predict and analyze the chemical constituents of tobacco during baking. The prediction results show that the model is feasible to predict the nicotine index at different stages of the baking process according to the color eigenvalues and texture eigenvalues of the tobacco leaves. The prediction results are in line with the actual situation, and the model has certain practical value.

References

Beura S., Majhi B., Dash R., 2015, Mammogram classification using two dimensional discrete wavelet transform and gray-level co-occurrence matrix for detection of breast cancer, Neurocomputing, 154, 1-14, DOI: 10.1016/j.neucom.2014.12.032

De Genna N.M., Ylioja T., Schulze A.E., Manta C., Douaihy A.B., Davis E.M., 2017, Electronic cigarette use among counseled tobacco users hospitalized in 2015, Journal of Addiction Medicine, 11, 1.

Gajewski M., Radzanowska J., Danilcenko H., Jariene, E., Cerniauskiene J., 2008, Quality of pumpkin cultivars in relation to sensory characteristics, Notulae Botanicae Horti Agrobotanici Cluj-Napoca, 36(1), 73-79.

Galiza R., Ferreira L., 2013, Standard pedestrian equivalent factors: new approach to analyzing pedestrian flow, Journal of Transportation Engineering, 139(2), 208-215, DOI:10.1061/(ASCE)TE.1943-5436.0000441

Huang X.B., Mao P.L., Dong X.P., Tang H.Y., 2014, A Hybrid Model for Short-Term Wind Speed Forecasting Based on Wavelet Analysis and RBF Neural Network, Unifying Electrical Engineering and Electronics Engineering, 238, 173-181. DOI:10.1007/978-1-4614-4981-2_19

Leventhal A.M., Strong D.R., Kirkpatrick M.G., Unger J.B., Sussman S., Riggs N.R., 2015, Association of electronic cigarette use with initiation of combustible tobacco product smoking in early adolescence, Jama, 314(7), 700-7.

Liang M., Hu X., 2015, Recurrent convolutional neural network for object recognition, In Proceedings of the IEEE Conference on Computer Vision and Pattern Recognition, 3367-3375.

Lin X., Zhu Q., Xuejun J.I., Zhang Z., Dong J., Cheng S., 2016, Correlation of chemical components with overall sensory quality of tobacco leaves in south anhui, Tobacco Science & Technology, 49(11), 42-55.

Nayak D.R., Dash R., Majhi B., 2016, Brain mr image classification using two-dimensional discrete wavelet transform and adaboost with random forests, Neurocomputing, 177(C), 188-197, DOI: 10.1016/j.neucom.2015.11.034

Romero A., Gatta C., Camps-Valls G., 2016, Unsupervised deep feature extraction for remote sensing image classification, IEEE Transactions on Geoscience and Remote Sensing, 54(3), 1349-1362.

Saadat S., Teknomo K., Fernandez P., 2012, Automation of tracking trajectories in a crowded situation, Fire Technology, 48(1), 73-90.

Spoerer C.J., Mcclure P., Kriegeskorte N., 2017, Recurrent convolutional neural networks: a better model of biological object recognition, Frontiers in Psychology, 8, 1551.

Sun W., Wang Y., 2018, Short-term wind speed forecasting based on fast ensemble empirical mode decomposition, phase space reconstruction, sample entropy and improved back-propagation neural network, Energy Conversion & Management, 157, 1-12.

Wang S., Zhang N., Wu L., Wang Y., 2016, Wind speed forecasting based on the hybrid ensemble empirical mode decomposition and ga-bp neural network method, Renewable Energy, 94, 629-636, DOI: 10.1016/j.renene.2016.03.103